Effects of the localized state inside the barrier on resonant tunneling in double-barrier quantum wells

Miao He and Ben-yuan Gu
Institute of Physics, Academia Sinica, P.O. Box 603, Beijing 100 080, People's Republic of China
(Received 5 September 1989)

We analyze the doping effects on resonant tunneling of a defect-layer sheet on the barrier in double-barrier quantum wells, using the effective-mass approximation and transfer-matrix approach. The potential for defects is taken to be a δ-function model potential. When the local-state level for the defects matches one of the quasibound state levels in the quantum well (QW), a strong coupling between them occurs. It splits and shifts the original resonant peaks in the transmission probability. In the opposite case, no splitting of the peaks is observed but an extra resonant peak corresponding to the defect state appears and the shifting of peaks occurs. The degree of coupling also depends on the position of the defect layer relative to the barrier-well interface. The closer to the interface the defect layer is, the stronger the coupling is. It shows that the localized state level and the position of the defect layer may be additional growth-control parameters and can be used to modify the energy structures of the QW.

I. INTRODUCTION

Resonant tunneling through quantum-well (QW) heterostructures has attracted considerable attention recently because of its possible application to ultrahigh-speed electronic devices.[1-6] Particle transmission through one QW, which is enclosed by two tunneling barriers, can exhibit sharp peaks when the incident-particle energies coincide with the energies of the quasibound states of the QW. The characteristics of quantum-well devices are closely related to the energy structures of the QW, generating considerable motivation in the investigation of the electronic states within the QW in recent years.

Recently, the effects of impurities, defects, and structural disorder on the resonant tunneling have been intensively studied[7-10] because both the characteristics of resonant tunneling diodes and the mechanism of the electron tunneling are strongly affected by the doping profile of the structures. In complete structures the resonant tunneling of electrons is coherent.[11] However, inelastic scattering in the well may destroy phase coherence and makes the electron lose its phase memory; it is said to tunnel sequentially.[12] The presence of scattering centers leads to a broadening and decrease of the resonant transmission peak,[13-16] equivalently to a broadening of the density of states in the well, and hence, also to a reduction of the peak-to-valley ratio. For the QW made by amorphous semiconductor materials both the experimental and theoretical investigations for resonant tunneling have also been presented by many investigators.[17-21]

Very recently, Cheng *et al.* presented a study on the effects of Si doping with different doping levels in AlAs barrier layers of AlAs/GaAs/AlAs double-barrier resonant tunneling diodes.[10] They observed that the peak-to-valley current ratios are not changed too much as the Si doping density increases in AlAs barriers. The resonant tunneling coherence is virtually unaffected by doping in the AlAs barriers over some ranges of the Si doping densities. They observed a shift of the peak in the resonant tunneling current and ascribed this shift to the band-bending effect.

Only a few theoretical studies concerned with effects of the localized states in barriers for the double-barrier quantum-well (DBQW) system on resonant tunneling are presented. More recently, Beltram and Capasso studied the interaction phenomena between deep levels of defect layers and minibands in semiconductor superlattices.[22] They presented calculations of the electronic states for a conventional heterojunction superlattice interleaved with a periodic array of deep centers located in the barrier layers. By appropriate choice of structural parameters strong mixing between defects and superlattice states takes place. Enhancement of the miniband widths by several orders of magnitude and the creation of new Bloch states within the band gap of the superlattices are found.

The aim of this work is to calculate the transmission probability of resonant tunneling through a barrier-well-barrier structure based on a model which takes into account the existence of a localized state inside one barrier and with the use of the effective-mass approximation and transfer-matrix approach. We present calculations showing that the localized state introduced in the barrier of the DBQW structure can have intriguing effects on the quasibound states for the QW. The strong coupling between the defects and the QW leads to rich phenomena such as the splitting of peaks, the shifting of peaks, the creation of a new peak, and the falling of the lower-energy peak into the band gap, or the incorporation of the higher-energy peak into the quasicontinuous states. The coupling or mixing of the states sensitively depends on the energy level of defects and on the location of the defect-layer sheet in the barrier. In Sec. II we shall briefly describe our model and the relevant formulas. The calculated results and analysis are given in Sec. III. Section IV presents some discussions.

II. MODEL AND FORMULAS

The analysis of the problem of a quantum particle through a DBQW containing a defect-layer sheet in the barrier needs some simplifying assumptions to be tractable. Since the one-dimensional model contains the essence of the problem, we shall consequently restrict our discussion to the one-dimensional case here. We consider monoenergetic electrons described in an effective-mass approximation. We neglect all complications such as band structure and charge pileup in QW, as well as transfer between longitudinal and transverse momentums, and only consider a defect-layer sheet located in the front barrier.

A schematic representation of the potential profile for a typical DBQW system is illustrated in Fig. 1. There exists a defect-layer sheet located at the position x_b in the barrier measured from the barrier-well interface. We focus on the investigation of the interaction between the localized state arising from the defect layer in the barrier and the quasibound states in the QW. As indicated by Beltram *et al.*,[22] since the qualitative results of the calculations are not influenced by the details of the potential chosen we shall use a δ function as a model potential to describe the defects.

We now consider an electron with energy E and effective mass m^* incident from the left side ($x<-a-b$) on a DBQW system, as shown in Fig. 1. We set the potential to the extreme left ($x<-a-b$), to the extreme right ($x>a+b$), and within the well to zero. The widths of barriers and the well are b and $2a$, respectively. We begin considering barrier I—a rectangular potential barrier of height $|e|V_0$ and width b. It is well known that the characteristics of a barrier can be completely determined by its 2×2 transfer matrix. In the case of no defect layer in barrier I we have[20]

$$\underline{M}(\text{barrier I})=\underline{M}(3\leftarrow2)\underline{M}(2\leftarrow1)\ , \tag{1a}$$

where

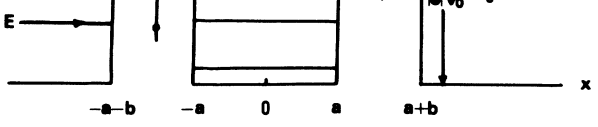

FIG. 1. Potential energy diagram for a double-barrier quantum well with a defect-layer sheet in the front barrier. The widths of barriers and the well are 30 and 55 Å, respectively. The height of the barriers is $|e|V_0=0.4$ eV. There are three energy levels for the quasibound states within the quantum well. The defect sheet is shown as a vertical line and is located at a position x_b measured from the barrier-well interface. The energy level for the defect state is shown as a dot.

$$\underline{M}(2\leftarrow1)=\underline{U}^{-1}(-\alpha_2(a+b))\times\underline{R}(ik_1m_2^*/\alpha_2m_1^*)\underline{U}(-ik_1(a+b))\ , \tag{1b}$$

$$\underline{M}(3\leftarrow2)=\underline{U}^{-1}(-ik_3a)\underline{R}(\alpha_2m_3^*/ik_3m_2^*)\underline{U}(-\alpha_2a)\ .$$

Similarly, for barrier II the transfer matrix has the following form:

$$\underline{M}(\text{barrier II})=\underline{M}(5\leftarrow4)\underline{M}(4\leftarrow3)\ , \tag{2a}$$

where

$$\underline{M}(4\leftarrow3)=\underline{U}^{-1}(\alpha_4a)\underline{R}(ik_3m_4^*/\alpha_4m_3^*)\underline{U}(ik_3a)\ , \tag{2b}$$

$$\underline{M}(5\leftarrow4)=\underline{U}^{-1}(ik_5(a+b))\times\underline{R}(\alpha_4m_5^*/ik_5m_4^*)\underline{U}(\alpha_4(a+b))\ .$$

And

$$\underline{R}(y)=\frac{1}{2}\begin{bmatrix}1+y & 1-y\\ 1-y & 1+y\end{bmatrix}\ , \tag{3}$$

$$\underline{U}(y)=\begin{bmatrix}e^y & 0\\ 0 & e^{-y}\end{bmatrix}\ ,$$

$$k_j^2=2m_j^*E/\hbar^2,\quad j=1,3,5 \tag{4}$$

$$\alpha_j^2=2m_j^*(|e|V_0-E)/\hbar^2,\quad j=2 \text{ and } 4\ .$$

Here the quantities with the index j refer to region j, seen in Fig. 1.

We now consider the modified barrier I containing a defect-layer sheet located at x_b. We assume that the potential for the defects has the form of a δ-type function: $\Omega_b\delta(x-x_b)$. Ω_b is the strength of the δ function. For negative Ω_b it represents an attractive interaction, in the opposite case, a repulsive one. This kind of potential reflects in the simplest way the fact that the defect state is strongly localized. Every δ potential in the barrier introduces one local state whose energy level is controlled by Ω_b: $E_b=|e|V_0-m^*\Omega_b^2/2\hbar^2$.[23] Through standard algebraic operation,[20] one can derive the transfer matrix corresponding to the defect as

$$\underline{M}_b(x_b,\Omega_b)=\underline{U}^{-1}(\alpha_2(-a-x_b))\underline{S}(\xi_b/2\alpha_2)\times\underline{U}(\alpha_2(-a-x_b))\ , \tag{5}$$

where

$$\underline{S}(y)=\begin{bmatrix}1-y & -y\\ y & 1+y\end{bmatrix}\ , \tag{6a}$$

and

$$\xi_b=-2m_2^*\Omega_b/\hbar^2\ . \tag{6b}$$

Thus, the transfer matrix for the modified barrier I can be written as

$$\underline{M}'(\text{barrier I})=\underline{M}(3\leftarrow2)\underline{M}_b(x_b,\Omega_b)\underline{M}(2\leftarrow1)\ . \tag{7}$$

At last, we can construct the total transfer matrix as the

product of the transfer matrices corresponding to barriers I and II

$$\underline{M}^{\text{tot}}(E,x_b,\Omega_b)=\underline{M}(\text{barrier II})\underline{M}'(\text{barrier I})\ . \quad (8)$$

Finally, the transmission amplitude of the system is related to the (2,2) element of $\underline{M}^{\text{tot}}$ as

$$t(E,x_b,\Omega_b)=1/M_{22}^{\text{tot}} \quad (9)$$

and the transmission probability is

$$T(E,x_b,\Omega_b)=\frac{v_R}{v_L}tt^*=\frac{k_5 m_1^*}{k_1 m_5^*}tt^*\ , \quad (10)$$

where v_L and v_R denote the velocity of the particle on the left- and right-hand sides of the DBQW, respectively. For a given x_b and Ω_b, we can calculate the transmission probability spectrum numerically.

III. CALCULATED RESULTS AND ANALYSIS

To have a quantitative feeling of the effects of defects in the barrier on resonant tunneling, it is necessary to perform numerical calculations in a special case. It should be pointed out that we are not able to make direct comparison with experimental data, but our model is a starting point to study the interaction phenomena between the localized state in the barrier and the quasibound states in the QW. For convenience we shall choose the set of parameters given by the paper of Gu *et al.*[20] The effective masses are the same as $m_j^*=0.2m_0$ for $j=1,2,\ldots,5$; m_0 is the mass of free electron. Widths of the barriers and the well are 30 and 55 Å, respectively. The height of the barriers is $|e|V_0=0.4$ eV. The main results are summarized below.

There exist two adjustable parameters for our model: the strength Ω_b of the δ function and the location x_b of the defect-layer sheet in the barrier.

First, we examine the effect of the defect-layer displacement x_b from the interface on resonant tunneling. Logarithm plots of the transmission probability as a function of incident electron energies with varying displacements but holding the strength Ω_b are shown in Fig. 2. Curves have been vertically offset for clarity. The dashed curves refer to the case of no defects ($\Omega_b=0$); here we find the results of Gu *et al.*[20] There are three peaks located at energies 40, 154, and 326 meV, respectively, which coincide, as expected, with the quasibound energy levels calculated for the finitely deep rectangular well. We set $\Omega_b=-4.5$ eV Å; it corresponds to a defect state with $E_b=134$ meV closer to the second peak E_2, as marked by an arrow in Fig. 2. Curves *a*, *b*, *c*, and *d* correspond to different locations of the defect layer: $x_b=0$, $b/4$, $b/2$, and $3b/4$, respectively. It is clearly seen that due to E_b being close to E_2 the coupling between them is strong. It leads to a split of the second peak around the original peak position in the opposite direction. As the defect layer displaces toward the interface, the peak splitting separation increases. It indicates that the coupling becomes stronger. Even though the first and third peaks are far away from E_b, they are still affected by this doping. Peak 1 shifts toward lower energy, but peak 3 shifts toward higher energy. As x_b decreases, coupling equivalently increases; the shift amount for peaks 1 and 3 may be so large that peak 1 falls into the gap below the conduction-band edge of the well, but peak 3 lifts up and over the height of the barrier and incorporates into the quasicontinuous energy states or some "virtual" levels. These kinds of virtual states caused by electron interference effects have also been observed.[24,25] Therefore, the number of peaks visible may be 2, 3, or 4, depending on the degrees of the coupling.

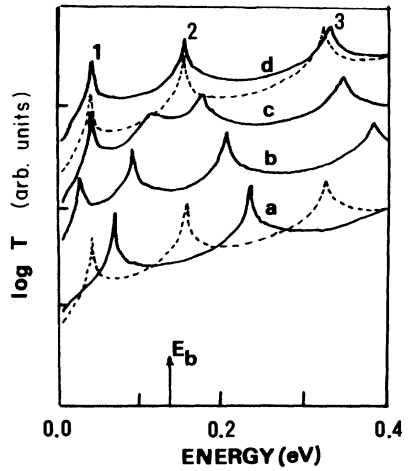

FIG. 2. Logarithmic plots of transmission probabilities vs incident electron energies for the system with increasing the defect-layer displacement x_b measured from the barrier-well interface but holding the energy level of the defect state, $E_b=134$ meV, as shown by an arrow. The dashed curves correspond to the case of no defect layer in the barrier. Curves *a*, *b*, *c*, and *d* correspond to different values of x_b: 0, $b/4$, $b/2$, and $3b/4$, respectively. Three original peaks are marked by 1, 2, and 3 in sequence from the lower to the higher energies. Curves have been vertically offset for clarity.

Figures 3(a)–3(c) show plots of the energy position of the peaks versus the displacement of the defect layer from the interface with different energies of the defect states: (a) $E_b=E_1$; (b) $E_b\approx E_2$; (c) $E_b=E_3$. It corresponds to the so-called "at resonant coupling" case where the energy level of the defect state is matched with one of the quasibound states in the QW. In Fig. 3 all of the dashed lines indicate the defect energy level being an invisible peak. For the visible peak E_b the curves are plotted by a solid line.

From the varying trend of these curves we can find some general regularities as follows: (1) Only the peak that closes E_b is split into dual resonant peaks located at two sides of the original peak due to the coupling interaction between the defect state and the quasibound state. It is called the case of at resonant coupling; (2) for the peaks far away from E_b they are also affected by this doping; the higher-energy peak above E_b shifts toward the higher energy, but the lower-energy peak below E_b shifts toward

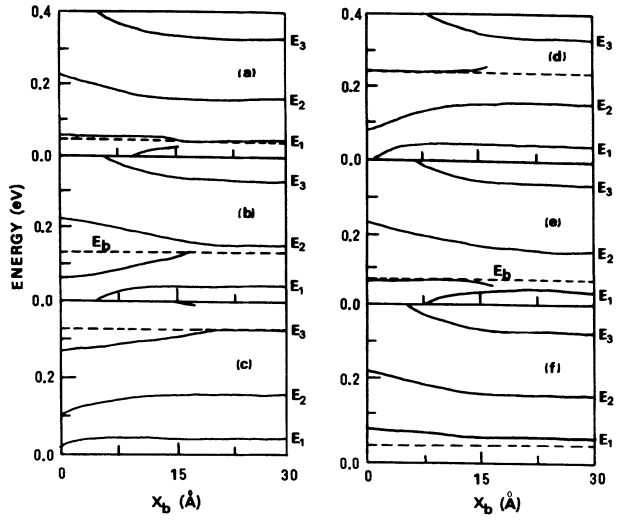

FIG. 3. Energy position of transmission probability peaks as a function of the defect-layer displacement from the interface, with different energy levels E_b for the defect states. All the dashed lines indicate the energy level for the defect states being the invisible peak. For the visible peak the line is plotted by a solid line. E_1, E_2, and E_3 are the positions in energy for original peaks 1, 2, and 3, respectively. The value of E_b corresponding to these figures is the following: (a) 40 meV ($=E_1$), (b) 134 meV, (c) 326 meV ($=E_3$), (d) 240 meV, (e) 72 meV, and (f) 0.0 meV.

lower energy; (3) as x_b decreases, i.e., the defect layer closes the interface, the coupling becomes stronger, the splitting separation of peaks increases, and the shift amount for the single peak relative to the original peak position also increases. The peak-to-valley ratio in the spectra is always changed due to the introduction of the defect-layer sheet. The increase of the valley transmission probability for the doping sample is also due to the coupling between the defect layer and the quasibound state in the QW. The decrease of the peak-to-valley ratio in the transmission probability spectrum indicates the coherence of the resonant tunneling is worse; (4) as the coupling increases continuously, peak 3 may lift over the height of the barrier and incorporate into the quasicontinuous energy states or virtual states. In contrast, peak 1 may fall below the conduction-band edge of the QW and becomes a gap state. It indicates that a gap state may be created due to introducing this defect layer; (5) the number of the resonance peaks depends on the degrees of the coupling; i.e., on x_b and on the energy level of defect states, how to close the interface and how to match with the quasibound states in the QW?

Figures 3(d)–3(f) show the case where the localized state for the defects lies between the two original quasibound levels of the QW: (d) $E_3 > E_b > E_2$, (e) $E_2 > E_b > E_1$, and (f) $E_1 > E_b \approx 0$, it is called the case of "off-resonant coupling." In this case there are some results considerably different from the at resonant coupling case. The first is that the peak split does not appear. The second is that an extra peak associated with E_b emerges in the strong coupling region. When the defect layer is centered in the barrier, the extra peak position slightly deviates from the E_b. In Fig. 3(f), no extra peak can be identified because the width of the coupled peak is very broad like a "bump."

We are now in a position to consider another variable: the energy level of the defect state. Figure 4 shows logarithmic plots of the transmission probability versus energy with different energy levels of the defect states but holding $x_b = b/2$. The dashed curves correspond to the case of no defects. Curves b–g correspond to $E_b = 347$, 326 ($=E_3$), 282, 154 ($=E_2$), 98, 40 ($=E_1$), and -73 meV, respectively. The energy levels of the defect states are also marked by arrows in Fig. 4. Curves are vertically offset for clarify. Referring to these spectral structures, we find that the above-mentioned regularities remain valid again.

To clarify this, we give plots of the peak position versus the strength of the δ function, as shown in Figs. 5(a)–5(c), corresponding to the case of the weak, inter-

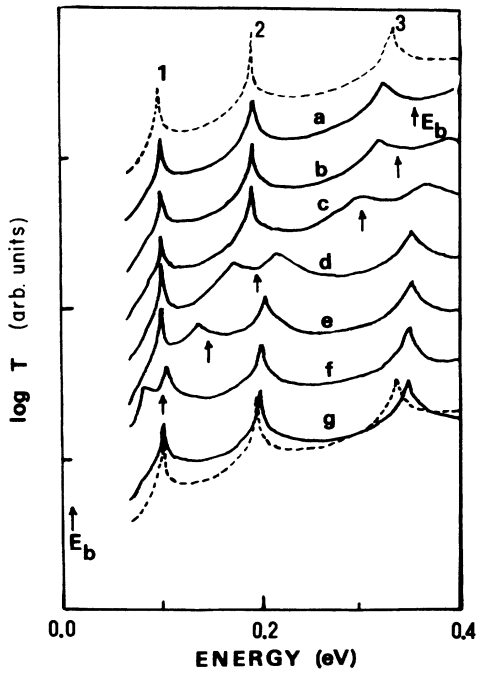

FIG. 4. Logarithmic transmission probabilities as a function of incident electron energies: without defects (dashed curves) and with defects which have varying energies but located at a fixed position, $x_b = b/2 = 15$ Å. The defect state energies E_b have been marked by arrows. Curves b, d, and f correspond to the at resonant coupling case: b, $E_b = E_3 = 326$ meV; d, $E_b = E_2 = 154$ meV; f, $E_b = E_1 = 40$ meV. However, curves a, c, and e describe the case of the off-resonant coupling: a, $E_b = 348$ meV; c, 282 meV; e, 98 meV. Final curve g corresponds to the case of the deep level of the defect state in the barrier: $E_b = -73$ meV. Curves are vertically offset for clarity.

mediate, and strong couplings, i.e., $x_b = 3b/4$, $b/2$, and $b/4$, respectively. The dashed curves present the parabolic relationship between the defect energy level and the strength parameter $|\Omega_b|$. In the weak coupling, as shown in Fig. 5(a), it is seen that all the peak positions are almost not changed even in the cross points A, B, and C defined by the condition: $E_b = E_3$, E_2, and E_1, respectively. No extra peak incorporates into the spectrum. That is due to the defect state being strongly localized; its wave function decays quickly with the distance. However, for the intermediate coupling, as seen in Fig. 5(b), at the energy cross points which correspond to the "at resonant coupling" case, the split of the peak occurs. In addition, in the region defined between A and C, the creation of one extra peak can be observed. This extra peak position in energy approaches to E_b generally, but sometime it is very difficult to assign its source because of the strong mixing effects. For the strong-coupling case, as shown in Fig. 5(c), the extra peak position may deviate far from E_b; there is no way to tell its original background. Near the cross point C, the interaction always forces the ground state to fall into the gap. On the other hand, at the cross point A, the interaction lifts the highest excited state up and incorporates it into the quasicontinuous states. It is interesting to note that when $|\Omega_b|$ is very large, the defect state energy level is very deep, like a strong attraction source in the barrier. It can lead to the split of the highest-energy peak and make a new quasibound state. This effect can be seen in both the intermediate- and strong-coupling regions, as shown in Figs. 5(b) and (c). The stronger the coupling is, the more obvious this effect is.

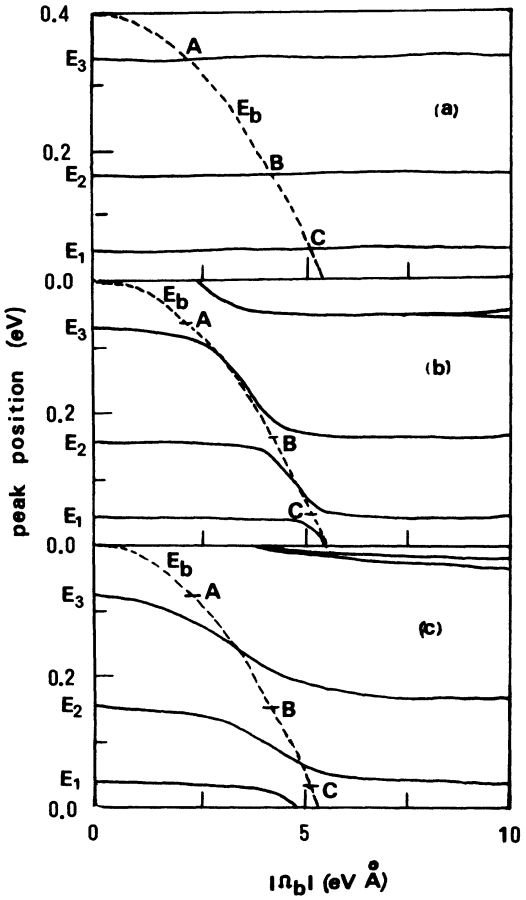

FIG. 5. Dependence of the transmission probability peak position in energy on the strength $|\Omega_b|$ of the δ function. Dashed curves describe the parabolic relation between E_b and Ω_b for the defect state. The cross points A, B, and C are defined by the condition: $E_b = E_3$, E_2, and E_1, respectively. (a), (b), and (c) correspond to the cases of the weak, intermediate, and strong couplings; the location of the defect layer is $3b/4$, $b/2$, and $b/4$, respectively.

When Ω_b is positive, corresponding to repulsive potential, only the scattering effect can be observed, the effect is similar to that of scattering centers in the well on resonant tunneling, as discussed by Gu *et al.*[20] In that case the effect of scattering is to lower the tunneling current and to shift toward higher energy, and broaden the peak of the resonance tunneling spectrum. Due to our symmetric structure, the results for doping in the rear barrier are the same as those obtained by the above calculations. For the case of both doping in the front and rear barriers, the effect is basically additional but more complicated.

IV. DISCUSSION

In the report recently presented by Cheng *et al.*,[10] they have observed the shift of the peak and valley voltages in the AlAs/GaAs/AlAs double-barrier resonant tunneling diodes with different doping levels in the AlAs barrier layers. They interpreted this shift to be caused by the band-bending effect. From our calculations above, we prefer to suggest that this shift may be generated by the strong coupling between the defect states in the barrier and the quasibound states in the QW.

The main findings of the present-day study for the DBQW system containing a defect layer in the barrier are similar to those of Beltram *et al.*[22] But they are concerned with a new superstructure consisting of a superlattice with the introduction of a periodic array of deep centers located in the barriers. Therefore, some results between our calculations and those of Beltram *et al.* are different. For our model, the coupling between the defects and the QW reaches maximum when the defect layer closes the interface, but in the system of Beltram *et al.* the interaction between deep levels of the defects and minibands in semiconductor superlattices is maximized when the energy levels of the defects are matched to those of the isolated wells and defect layers centered in the barriers. In fact, in that case the overlapping effect of wave functions between the defect and superlattice is maximum.

It is also interesting to note that the effects of a localized state formed inside the barrier on resonant tunneling for the DBQW system are similar to the case of coupled double-quantum-well structures where two adjacent quantum wells are separated by an ultrathin barrier that allows tunneling of electrons between the wells, as reported by Nakagawa *et al.* recently.[26] Dual resonant peaks

are obtained in their current-voltage characteristics. The peak separation is interpreted to be the coupling between the two wells. The energy splitting decreases as the thickness of the ultrathin barrier increases. These features are in good agreement with our calculated results.

Our model structures discussed here may be produced by the deposition of sheets of shallow impurities at high surface concentration as shown by Hjalmarson.[27] As described by Beltram *et al.*,[22] the actual realization of these structure is not very demanding for modern growth techniques such as state-of-the-art molecular-beam epitaxy. More recently Schubert *et al.*[28] have grown δ-doped *n-i-p-i* superlattices consisting of single atomic planes of shallow dopants via the "impurity-growth mode." Their experiments show that by proper control of the growth temperature the impurities were confined to single monolayers without degrading the crystallinity of the material. By using this technique the creation of a defect-layer sheet might be achieved.

In summary, we have presented the detailed studies of the effects of a localized state in the barrier on the resonant tunneling for the DBQW system. Our calculated results show that a surprising variety of coupling phenomena between the defect state and the quasibound states in the QW can be observed. From our calculations we are able to control the electronic energy structures for the QW by the introduction of defects in the barriers. It may provide new degrees of freedom for the optimal design of the QW devices and open a new way to improve the characteristics of the QW devices.

ACKNOWLEDGMENTS

The authors would like to thank Professor K. Q. Lu for continuing encouragement and constant support during the course of this work. This work was supported by the Chinese National Science Foundation.

[1]L. Esaki, J. Phys. (Paris) Colloq. **45**, C5-3 (1984).
[2]H. C. Liu and D. D. Coon, Appl. Phys. Lett. **50**, 1246 (1987).
[3]T. C. L. G. Sollner, W. D. Goodhue, P. E. Tannenwald, C. D. Parker, and D. D. Peck, Appl. Phys. Lett. **43**, 588 (1983).
[4]T. C. L. G. Sollner, E. D. Brown, W. D. Goodhue, and H. Q. Le, Appl. Phys. Lett. **50**, 332 (1987).
[5]For example, see *Two Dimensional Systems, Heterostructures and Superlattices,* edited by G. Bauer, F. Kuchar, and H. Heinrich (Springer-Verlag, New York, 1984).
[6]F. Capasso, K. Mohammed, and A. Y. Cho, IEEE, J. Quantum Electron **QE-22**, 1853 (1986).
[7]S. Muto, T. Inata, H. Ohnishi, N. Yokoyama, and S. Hiyamizu, Jpn. J. Appl. Phys. Pt. 1 **25**, 577 (1986).
[8]C. I. Huang, M. J. Paulus, C. A. Bozada, S. C. Dudley, K. R. Evans, C. E. Stutz, R. L. Jones, and M. E. Cheney, Appl. Phys. Lett. **51**, 121 (1988).
[9]E. Wolak, K. L. Lear, P. M. Pitner, E. S. Hellman, B. G. Park, T. Weil, J. S. Harris, Jr., and D. Thomas, Appl. Phys. Lett. **53**, 201 (1988).
[10]P. Cheng and J. S. Harris, Jr., Appl. Phys. Lett. **55**, 572 (1989).
[11]B. Ricco and M. Ya Azbel, Phys. Rev. B **29**, 1970 (1984).
[12]S. Luryi, Appl. Phys. Lett. **47**, 490 (1985).
[13]A. D. Stone and P. A. Lee, Phys. Rev. Lett. **54**, 1196 (1985).
[14]M. Jonson and A. Grincwajg, Appl. Phys. Lett. **51**, 1729 (1987).
[15]P. J. Price, in *Proceedings of the Workshop on Physics of Superlattices and Quantum Wells, Shanghai, China, 1988,* edited by C. H. Tsai, X. Wang, X. C. Shen, and X. L. Lei (World Scientific, Singapore, 1989), p. 22.
[16]M. Büttiker, IBM J. Res. Dev. **32**, 63 (1988).
[17]S. Miyazaki, Y. Ihara, and M. Hirose, Phys. Rev. Lett. **59**, 125 (1987).
[18]I. Pereyra, M. P. Carreno, R. A. Onmori, C. A. Sassaki, A. M. Andrade, and F. Alvarez, J. Non-Cryst. Solids **97&98**, 871 (1987).
[19]P. A. Schulz and C. E. T. Gonçalves da Silva, Phys. Rev. B **38**, 10 718 (1988).
[20]B. Y. Gu, C. Coluzza, M. Mangiantini, and A. Frova, J. Appl. Phys. **65**, 3510 (1989).
[21]B. Y. Gu, C. Coluzza, and M. Mangiantini, Superlatt. Microstruct. **6**, 153 (1989).
[22]F. Beltram and F. Capasso, Phys. Rev. B **38**, 3580 (1988).
[23]V. I. Kogan and M. Galitskiy, *Problems in Quantum Mechanics* (Prentice-Hall, Englewood Cliffs, NJ, 1956), p. 59.
[24]R. C. Potter and A. A. Lakhani, Appl. Phys. Lett. **52**, 1349 (1988).
[25]S. Sen, F. Capasso, A. C. Gossard, R. A. Spach, A. Hutchinson, and S. N. G. Chu, Appl. Phys. Lett. **51**, 1428 (1987).
[26]T. Nakagawa, A. Ishida, T. Kojima, and K. Ohta, Superlatt. Microstruct. **5**, 231 (1989).
[27]H. P. Hjalmarson, J. Vac. Sci. Technol. **21**, 524 (1982).
[28]E. F. Schubert, J. E. Cunningham, and W. T. Tsang, Phys. Rev. B **36**, 1348 (1987).